Shock and Vibration 20 (2013) 227–246
DOI 10.3233/SAV-2012-00740
IOS Press

Experimental study of H_∞ control of flexible plate with time delay

Tong Zhao, Long-Xiang Chen and Guo-Ping Cai*
Department of Engineering Mechanics, State Key Laboratory of Ocean Engineering, Shanghai Jiaotong University, Shanghai, China

Received 13 February 2012
Revised 14 May 2012

Abstract. This paper presents theoretical and experimental studies of H_∞ control of a flexible plate with time delay. A matrix inequality used for stability analysis is proposed and proved by using the Lyapunov-Krasovskii functional and free-weighting matrix. An H_∞ controller is designed based on the matrix inequality and by using the parameter-adjusting method. Three control scenarios are discussed in detail by transforming the problem into parameters optimization: (i) controller design when maximum time delay of the system is known; (ii) allowable time delay when controller is known; (iii) the biggest allowable time delay to guarantee system stability when controller is unknown. Numerical simulations and experiments are also given to demonstrate the validity and feasibility of the proposed methods in this paper.

Keywords: Flexible plate, matrix inequality, H_∞ control, time delay, experiment

1. Introduction

In dynamic modeling and active control of structures, errors may occur in the modeling process due to uncertainty of physical properties and boundary conditions of the structure, and signal noise and external disturbance may also affect control effectiveness at control implementation. So the controller designed should be of strong robustness to eliminate the effect of negative factors on control effectiveness. Among modern control systems, robust control method is robust to the variance of structural intrinsic parameters and external disturbance, and has been getting more and attention in the active control of structures [1–8].

Time delay inevitably exists in active control systems. Many factors, such as system variables measuring, controller calculating, and actuators building up the required control force, may result in non-synchronizing control force, which may cause degradation of control efficiency, or even instability of the system [9]. So far time delay problems are mainly investigated in mathematics and control systems, and most studies are focused on stability or the maximum allowable time delay to maintain time-delay systems stable. For active control of structures, some treating methods were proposed to deal with time delay, such as the Taylor series [10], the technique of phase shift [11], the advance estimation of state variables [12], etc. But these methods are only applicable for systems with very small time delay, and work awkwardly for systems with large delays. Lately, Cai and Huang [13,14] worked out a new method for time delay, in which the active controller is designed directly from the time-delay differential equation and no approximation and estimation are made in the process of control design, and system performance and stability are easily guaranteed. The proposed method in [13,14] is applicable for both small time delay and large time delay problems, which is experimentally verified by working on different flexible structures [15,16].

*Corresponding author: Tong Zhao, Department of Engineering Mechanics, State Key Laboratory of Ocean Engineering, Shanghai Jiaotong University, Shanghai 200240, China. E-mail: caigp@sjtu.edu.cn.

ISSN 1070-9622/13/$27.50

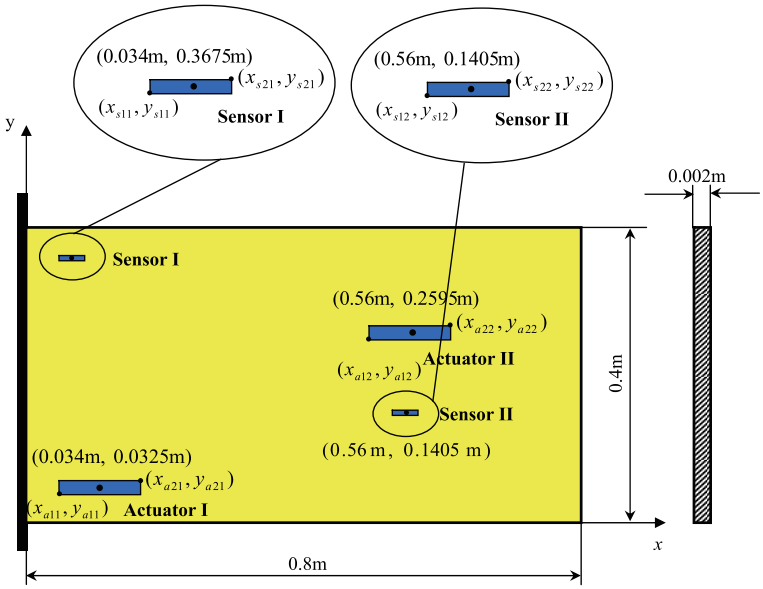

Fig. 1. Structural model of flexible plate.

Hu et al. [17,18] then modified the method in [14] and proposed a treating method for slowly time-varying delay systems. There also have been many studies on the time-delay robust control of structures. For example, Du and Zhang [19], with time delay as an input, worked on an approach to designing an H_∞ controller to attenuate the vibration of seismically-excited buildings. Chen and Tian [20] proposed a new approach for delay-dependent robust H_∞ stability analysis and control synthesis of uncertain systems with time-varying delays. Alberto Cavallo et al. [21] considered a control law for the active vibration control of mechanical flexible systems, and the proposed strategy can minimize an H_∞ index and attain a favorable stabilizing controller with bandpass frequency shape. Chung et al. [22] developed a time-delay control algorithm to solve the practical problem that time-delay caused unsynchronized application of the control forces which may not only degrade the performance of the control system but also even induce instability to the dynamic system. Yuen and Beck [23] presented a reliability-based output feedback control methodology for controlling the dynamic response of systems that are represented by linear state-space models. It should be mentioned herein that, although many effects have been made on the time-delay techniques, most work is on the theoretical basis and little on the experiment. For robust controllers taking account of time delay, to the authors' knowledge, there has been no experimental study so far.

This paper theoretically and experimentally studies the H_∞ control of a flexible plate with time delay. A matrix inequality for stability analysis is proposed and proved by using the Lyapunov-Krasovskii functional and free-weighting matrix. An H_∞ controller is presented based on the matrix inequality. This paper goes as follows. Section 2 presents the motion equation of the flexible plate; Section 3 provides the matrix inequality and H_∞ controller; Section 4 presents the discusses three scenarios: (i) controller design with known maximum time delay; (ii) allowable time delay with known controller; (iii) the biggest allowable time delay to maintain system stability with unknown controller. Section 5 talks about numerical simulations and experiment studies. Finally, Section 6 concludes with a few remarks.

2. Equation of motion

Transverse vibration of a flexible cantilever plate is considered, as shown in Fig. 1. Assume that q piezoelectric (PZT) actuators are used for vibration control of the plate. Using the orthogonality of modal function and truncating the first n modes of the plate, the dynamic equation of the plate may be written as [16,24]

$$\ddot{\hat{\mathbf{\Phi}}}(t) + \hat{\mathbf{C}}\dot{\hat{\mathbf{\Phi}}}(t) + \hat{\mathbf{K}}\hat{\mathbf{\Phi}}(t) = \hat{\mathbf{H}}\mathbf{V}(t) \tag{1}$$

where $\hat{\mathbf{\Phi}}(t) = [\phi_1, \phi_2, \cdots, \phi_n]^{\mathrm{T}}$ is the n-dimensional vector of modal coordinate, ϕ_j represent the modal coordinate of the j-th mode of plate, T denotes the transpose of a matrix or vector, n is the number of degree of freedom of the plate; $\hat{\mathbf{C}} = \mathrm{diag}(2\zeta_1\omega_1, 2\zeta_2\omega_2, \cdots, 2\zeta_n\omega_n)$ is the $n \times n$ damping matrix of the plate, ζ_j and ω_j are the damping ratio and natural frequency of the plate, respectively; $\hat{\mathbf{K}} = \mathrm{diag}(\omega_1^2, \omega_2^2, \cdots, \omega_n^2)$ is the $n \times n$ stiffness matrix of the plate; $\hat{\mathbf{H}} = [\hat{\mathbf{H}}_1, \hat{\mathbf{H}}_2, \cdots, \hat{\mathbf{H}}_q]$ is an $n \times q$ matrix denoting the positions of actuators, $\hat{\mathbf{H}}_i = \hat{\mathbf{M}}^{-1}[\mathrm{piezo}_1^i, \mathrm{piezo}_2^i, \cdots, \mathrm{piezo}_n^i]^{\mathrm{T}}$ is an $n \times 1$ vector, $\hat{\mathbf{M}}$ is the $n \times n$ modal mass matrix of the plate. The coefficient of PZT actuator, piezo_j^i, is given by [16,24]

$$\begin{aligned}\mathrm{piezo}_j^i = -\Bigg\{ & C_0^i \frac{d_{31i}}{h_{ai}} \left[\int_{y_{a1i}}^{y_{a2i}} W_{jx}(x_{a2i}, y)\mathrm{d}y - \int_{y_{a1i}}^{y_{a2i}} W_{jx}(x_{a1i}, y)\mathrm{d}y \right] \\ & + C_0^i \frac{d_{31i}}{h_{ai}} \left[\int_{x_{a1i}}^{x_{a2i}} W_{jy}(x, y_{a2i})\mathrm{d}x - \int_{x_{a1i}}^{x_{a2i}} W_{jy}(x, y_{a1i})\mathrm{d}x \right] \Bigg\}\end{aligned} \tag{2}$$

where $W_j(x, y)$ represent the modal function of the j-th mode of plate, $W_{jx} = \partial W_j/\partial x$ and $W_{jy} = \partial W_j/\partial y$; d_{31i} and h_{ai} are the bending strain constant and thickness of the i-th PZT actuator, respectively; (x_{a1i}, y_{a1i}) and (x_{a2i}, y_{a2i}) are the down-left and top-right coordinates of the i-th PZT actuator in the *o-xy* system, respectively, as shown in Fig. 1. The parameter C_0^i in Eq. (3) is the mechanical-electrical coupling coefficient between the i-th PZT actuator and the plate, the expression of C_0^i can be found in [16,24].

In the state space representation, Eq. (2) becomes

$$\dot{\mathbf{x}}(t) = \mathbf{A}\mathbf{x}(t) + \mathbf{B}_2\mathbf{V}(t) \tag{3}$$

where $\mathbf{x}(t) = \begin{bmatrix} \hat{\mathbf{\Phi}}(t) \\ \dot{\hat{\mathbf{\Phi}}}(t) \end{bmatrix}$, $\mathbf{A} = \begin{bmatrix} \mathbf{0} & \mathbf{I} \\ -\hat{\mathbf{K}} & -\hat{\mathbf{C}} \end{bmatrix}$ and $\mathbf{B}_2 = \begin{bmatrix} \mathbf{0} \\ \hat{\mathbf{H}} \end{bmatrix}$.

3. Matrix inequality and H_∞ controller

Considering time delay τ and external disturbance $\mathbf{w}(t)$ in control input, and the controllable output $\mathbf{z}(t)$ of the system, the control problem of the plate can be written as

$$\begin{cases} \dot{\mathbf{x}}(t) = \mathbf{A}\mathbf{x}(t) + \mathbf{B}_1\mathbf{w}(t) + \mathbf{B}_2\mathbf{V}(t-\tau) \\ \mathbf{z}(t) = \mathbf{C}_1\mathbf{x}(t) + \mathbf{D}_{12}\mathbf{V}(t-\tau) + \mathbf{D}_{11}\mathbf{w}(t) \end{cases} \tag{4}$$

where $\mathbf{B}_1 = \mathbf{B}_2$ and $0 \leqslant \tau \leqslant \bar{\tau}$, $\bar{\tau}$ is the upper bound of time delay; $\mathbf{C}_1$, $\mathbf{D}_{12}$ and $\mathbf{D}_{11}$ are the coefficient matrices of appropriate dimensions.

The following memoryless controller is used for the system

$$\mathbf{V}(t) = \mathbf{K}\mathbf{x}(t) \tag{5}$$

where $\mathbf{K}$ is the control feedback gain matrix. Substituting Eq. (5) into Eq. (4), we have

$$\begin{cases} \dot{\mathbf{x}}(t) = \mathbf{A}\mathbf{x}(t) + \mathbf{B}_1\mathbf{w}(t) + \mathbf{B}_K\mathbf{x}(t-\tau) \\ \mathbf{z}(t) = \mathbf{C}_1\mathbf{x}(t) + \mathbf{D}_K x(t-\tau) + \mathbf{D}_{11}\mathbf{w}(t) \end{cases} \tag{6}$$

where $\mathbf{B}_K = \mathbf{B}_2\mathbf{K}$ and $\mathbf{D}_K = \mathbf{D}_{12}\mathbf{K}$.

3.1. Matrix inequality

Here a matrix inequality is proposed for stability analysis and controller design. The following two lemmas will be used in the derivation and proof of the matrix inequality.

Lemma 1. [25] *Schur Complements: For a symmetric matrix* $\mathbf{S} = \mathbf{S}^{\mathrm{T}} = \begin{bmatrix} \mathbf{S}_{11} & \mathbf{S}_{12} \\ \mathbf{S}_{12}^{\mathrm{T}} & \mathbf{S}_{22} \end{bmatrix}$, *where* $\mathbf{S}_{11} = \mathbf{S}_{11}^{\mathrm{T}}$ *and* $\mathbf{S}_{22} = \mathbf{S}_{22}^{\mathrm{T}}$, *the following three conditions are equivalent*

$$\begin{cases} (i) & \mathbf{S} < 0 \\ (ii) & \mathbf{S}_{11} < 0 \; and \; \mathbf{S}_{22} - \mathbf{S}_{12}^{\mathrm{T}} \mathbf{S}_{11}^{-1} \mathbf{S}_{12} < 0 \\ (iii) & \mathbf{S}_{22} < 0 \; and \; \mathbf{S}_{11} - \mathbf{S}_{12} \mathbf{S}_{22}^{-1} \mathbf{S}_{12}^{\mathrm{T}} < 0 \end{cases} \tag{7}$$

Lemma 2. [26] *There exists a symmetric matrix* $\tilde{\mathbf{X}}$ *such that*

$$\begin{bmatrix} \mathbf{P}_1 + \tilde{\mathbf{X}} & \mathbf{Q}_1 \\ * & \mathbf{R}_1 \end{bmatrix} < 0, \quad \begin{bmatrix} \mathbf{P}_2 - \tilde{\mathbf{X}} & \mathbf{Q}_2 \\ * & \mathbf{R}_2 \end{bmatrix} < 0 \tag{8}$$

if and only if

$$\begin{bmatrix} \mathbf{P}_1 + \mathbf{P}_2 & \mathbf{Q}_1 & \mathbf{Q}_2 \\ * & \mathbf{R}_1 & 0 \\ * & * & \mathbf{R}_2 \end{bmatrix} < 0 \tag{9}$$

By using the above two lemmas and the free-weighting matrix given in [3,5], the following theorem presents the delay-dependent sufficient condition for the existence of theH_∞ controller.

Theorem 1. *Given* $\bar{\tau}$, *if there exist real matrices* $\mathbf{P} > 0$, $\mathbf{R} > 0$, $\mathbf{Q} > 0$, *and the two free-weighting matrices* $\mathbf{N}_1$ *and* $\mathbf{N}_2$, *satisfying the matrix inequality*

$$\boldsymbol{\Xi} = \begin{bmatrix} \boldsymbol{\Xi}_{11} & \boldsymbol{\Xi}_{12} & \mathbf{P}\mathbf{B}_1 & \bar{\tau}\mathbf{A}^{\mathrm{T}} & \bar{\tau}\mathbf{N}_1 & \mathbf{C}_1^{\mathrm{T}} \\ * & \boldsymbol{\Xi}_{22} & \mathbf{0} & \bar{\tau}\mathbf{B}_K^{\mathrm{T}} & \bar{\tau}\mathbf{N}_2 & \mathbf{D}_K^{\mathrm{T}} \\ * & * & -\gamma^2\mathbf{I} & \bar{\tau}\mathbf{B}_1^{\mathrm{T}} & \mathbf{0} & \mathbf{D}_{11}^{\mathrm{T}} \\ * & * & * & -\bar{\tau}\mathbf{R}^{-1} & \mathbf{0} & \mathbf{0} \\ * & * & * & * & -\bar{\tau}\mathbf{R} & \mathbf{0} \\ * & * & * & * & * & -\mathbf{I} \end{bmatrix} < 0 \tag{10}$$

where

$$\boldsymbol{\Xi}_{11} = \mathbf{P}\mathbf{A} + \mathbf{A}^{\mathrm{T}}\mathbf{P} + \mathbf{Q} + \mathbf{N}_1 + \mathbf{N}_1^{\mathrm{T}}, \quad \boldsymbol{\Xi}_{12} = \mathbf{P}\mathbf{B}_K - \mathbf{N}_1 + \mathbf{N}_2^{\mathrm{T}}, \quad \boldsymbol{\Xi}_{22} = -\mathbf{Q} - \mathbf{N}_2 - \mathbf{N}_2^{\mathrm{T}}$$

the closed-loop system Eq. (6) *is asymptotically stable with* H_∞ *performance index* γ *for any time delay* τ *satisfying* $0 \leqslant \tau \leqslant \bar{\tau}$.

Proof. By using the Leibniz-Newton formula, we have

$$\mathbf{x}(t-\tau) = \mathbf{x}(t) - \int_{t-\tau}^{t} \dot{\mathbf{x}}(s)\mathrm{d}s \tag{11}$$

For any $\mathbf{N}_1$ and $\mathbf{N}_2$ of appropriate dimensions, by using Eq. (11), we have

$$2[\mathbf{x}^{\mathrm{T}}(t)\mathbf{N}_1 + \mathbf{x}^{\mathrm{T}}(t-\tau)\mathbf{N}_2] \times [\mathbf{x}(t) - \mathbf{x}(t-\tau) - \int_{t-\tau}^{t} \dot{\mathbf{x}}(s)\mathrm{d}s] = 0 \tag{12}$$

Let $\boldsymbol{\eta}_1(t) = [\mathbf{x}^{\mathrm{T}}(t) \quad \mathbf{x}^{\mathrm{T}}(t-\tau)]^{\mathrm{T}}$, for a symmetric matrix $\mathbf{X} = \begin{bmatrix} \mathbf{X}_{11} & \mathbf{X}_{12} \\ * & \mathbf{X}_{22} \end{bmatrix} \geqslant 0$ of appropriate dimension, since $\bar{\tau} \geqslant \tau$, we have

$$\bar{\tau}\boldsymbol{\eta}_1^{\mathrm{T}}(t)\mathbf{X}\boldsymbol{\eta}_1(t) - \int_{t-\tau}^{t} \boldsymbol{\eta}_1^{\mathrm{T}}(t)\mathbf{X}\boldsymbol{\eta}_1(t)\mathrm{d}s = (\bar{\tau} - \tau)\boldsymbol{\eta}_1^{\mathrm{T}}(t)\mathbf{X}\boldsymbol{\eta}_1(t) \geqslant 0 \tag{13}$$

The Lyapunov-Krasovskii functional is chosen as [3,5]

$$V = \mathbf{x}^{\mathrm{T}}(t)\mathbf{P}\mathbf{x}(t) + \int_{t-\tau}^{t} \mathbf{x}^{\mathrm{T}}(s)\mathbf{Q}\mathbf{x}(s)\mathrm{d}s + \int_{-\bar{\tau}}^{0}\int_{t+\theta}^{t} \dot{\mathbf{x}}^{\mathrm{T}}(s)\mathbf{R}\dot{\mathbf{x}}(s)\mathrm{d}s\mathrm{d}\theta \geqslant 0 \tag{14}$$

where $\mathbf{P} = \mathbf{P}^{\mathrm{T}} > 0$, $\mathbf{Q} = \mathbf{Q}^{\mathrm{T}} > 0$ and $\mathbf{R} = \mathbf{R}^{\mathrm{T}} > 0$ are all positive definite matrices.

The derivative of Eq. (14) along the trajectory of Eq. (6) is given by

$$\begin{aligned}\dot{V} = {} & \mathbf{x}^{\mathrm{T}}(t)[\mathbf{A}^{\mathrm{T}}\mathbf{P} + \mathbf{P}\mathbf{A}]\mathbf{x}(t) + 2\mathbf{x}^{\mathrm{T}}(t-\tau)\mathbf{P}\mathbf{B}_K\dot{\mathbf{x}}(t) + \mathbf{x}^{\mathrm{T}}(t)\mathbf{P}\mathbf{B}_1\mathbf{w}(t) + \mathbf{w}^{\mathrm{T}}(t)\mathbf{B}_1^{\mathrm{T}}\mathbf{P}\mathbf{x}(t) \\ & + \mathbf{x}^{\mathrm{T}}(t)\mathbf{Q}\mathbf{x}(t) - \mathbf{x}^{\mathrm{T}}(t-\tau)\mathbf{Q}\mathbf{x}(t-\tau) + \bar{\tau}\Gamma - \int_{t-\bar{\tau}}^{t} \dot{\mathbf{x}}^{\mathrm{T}}(s)\mathbf{R}\dot{\mathbf{x}}(s)\mathrm{d}s\end{aligned} \tag{15}$$

where

$$\Gamma = \boldsymbol{\eta}_2^{\mathrm{T}}(t)(\boldsymbol{\Gamma}_1^{\mathrm{T}}\mathbf{R}\boldsymbol{\Gamma}_1)\boldsymbol{\eta}_2(t), \quad \boldsymbol{\Gamma}_1 = [\,\mathbf{A} \;\; \mathbf{B}_K \;\; \mathbf{B}_1\,]$$

with

$$\boldsymbol{\eta}_2(t) = [\,\boldsymbol{\eta}_1^{\mathrm{T}}(t) \;\; \mathbf{w}^{\mathrm{T}}(t)\,]^{\mathrm{T}} = [\,\mathbf{x}^{\mathrm{T}}(t) \;\; \mathbf{x}^{\mathrm{T}}(t-\tau) \;\; \mathbf{w}^{\mathrm{T}}(t)\,]^{\mathrm{T}}$$

Using Eqs (12) and (13), we have

$$\begin{aligned}\dot{V} \leqslant {} & \dot{V} + \left\{2[\mathbf{x}^{\mathrm{T}}(t)\mathbf{N}_1 + \mathbf{x}^{\mathrm{T}}(t-\tau)\mathbf{N}_2] \times [\mathbf{x}(t) - \mathbf{x}(t-\tau) - \int_{t-\tau}^{t} \dot{\mathbf{x}}(s)\mathrm{d}s]\right\} \\ & + \left[\bar{\tau}\boldsymbol{\eta}_1^{\mathrm{T}}(t)\mathbf{X}\boldsymbol{\eta}_1(t) - \int_{t-\tau}^{t} \boldsymbol{\eta}_1^{\mathrm{T}}(t)\mathbf{X}\boldsymbol{\eta}_1(t)\mathrm{d}s\right] - \left[\gamma^2\mathbf{w}^{\mathrm{T}}(t)\mathbf{w}(t) - \gamma^2\mathbf{w}^{\mathrm{T}}(t)\mathbf{w}(t)\right]\end{aligned} \tag{16}$$

Substituting Eq. (15) into the right-hand side of Eq. (16) and considering $\int_{t-\bar{\tau}}^{t} \dot{\mathbf{x}}^{\mathrm{T}}(s)\mathbf{R}\dot{\mathbf{x}}(s)\mathrm{d}s \geqslant \int_{t-\tau}^{t} \dot{\mathbf{x}}^{\mathrm{T}}(s)\mathbf{R}\dot{\mathbf{x}}(s)\mathrm{d}s$, Eq. (16) can be simplified as

$$\dot{V} \leqslant \boldsymbol{\eta}_2^{\mathrm{T}}(t)(\Sigma + \bar{\tau}\boldsymbol{\Gamma}_1^{\mathrm{T}}\mathbf{R}\boldsymbol{\Gamma}_1)\boldsymbol{\eta}_2(t) - \int_{t-\tau}^{t} \boldsymbol{\eta}_3^{\mathrm{T}}(t,s)\boldsymbol{\Psi}\boldsymbol{\eta}_3(t,s)\mathrm{d}s + \gamma^2\mathbf{w}^{\mathrm{T}}(t)\mathbf{w}(t) \tag{17}$$

where

$$\boldsymbol{\eta}_3(t) = [\,\mathbf{x}^{\mathrm{T}}(t) \;\; \mathbf{x}^{\mathrm{T}}(t-\tau) \;\; \dot{\mathbf{x}}^{\mathrm{T}}(s)\,]^{\mathrm{T}}, \quad \boldsymbol{\Psi} = \begin{bmatrix} \mathbf{X}_{11} & \mathbf{X}_{12} & \mathbf{N}_1 \\ * & \mathbf{X}_{22} & \mathbf{N}_2 \\ * & * & \mathbf{R} \end{bmatrix}$$

$$\boldsymbol{\Sigma} = \begin{bmatrix} \boldsymbol{\Xi}_{11} + \bar{\tau}\mathbf{X}_{11} & \mathbf{P}\mathbf{B}_K - \mathbf{N}_1 + \mathbf{N}_2^{\mathrm{T}} + \bar{\tau}\mathbf{X}_{12} & \mathbf{P}\mathbf{B}_1 \\ * & -\mathbf{Q} - (\mathbf{N}_2 + \mathbf{N}_2^{\mathrm{T}}) + \bar{\tau}\mathbf{X}_{22} & \mathbf{0} \\ * & * & -\gamma^2\mathbf{I} \end{bmatrix}$$

Below we will prove Theorem 1 from two aspects. First, we will prove that the close-loop system Eq. (6) is asymptotically stable for $0 \leqslant \tau \leqslant \bar{\tau}$ if Eq. (10) is satisfied.

Assume $\mathbf{w}(t) = 0$ for $t > 0$, Eq. (17) becomes

$$\dot{V} \leqslant \boldsymbol{\eta}_1^{\mathrm{T}}(t)(\hat{\boldsymbol{\Sigma}} + \bar{\tau}\hat{\boldsymbol{\Gamma}}_1^{\mathrm{T}}\mathbf{R}\hat{\boldsymbol{\Gamma}}_1)\boldsymbol{\eta}_1(t) - \int_{t-\tau}^{t} \boldsymbol{\eta}_3^{\mathrm{T}}(t,s)\boldsymbol{\Psi}\boldsymbol{\eta}_3(t,s)\mathrm{d}s \tag{18}$$

where

$$\hat{\boldsymbol{\Sigma}} = \begin{bmatrix} \boldsymbol{\Xi}_{11} + \bar{\tau}\mathbf{X}_{11} & \mathbf{P}\mathbf{B}_K - \mathbf{N}_1 + \mathbf{N}_2^{\mathrm{T}} + \bar{\tau}\mathbf{X}_{12} \\ * & -\mathbf{Q} - (\mathbf{N}_2 + \mathbf{N}_2^{\mathrm{T}}) + \bar{\tau}\mathbf{X}_{22} \end{bmatrix} = \bar{\tilde{\boldsymbol{\Sigma}}} + \bar{\tau}\mathbf{X}, \quad \hat{\boldsymbol{\Gamma}}_1 = [\,\mathbf{A} \;\; \mathbf{B}_K\,]$$

with

$$\bar{\hat{\boldsymbol{\Sigma}}} = \begin{bmatrix} \boldsymbol{\Xi}_{11} & \mathbf{P}\mathbf{B}_K - \mathbf{N}_1 + \mathbf{N}_2^{\mathrm{T}} \\ * & -\mathbf{Q} - (\mathbf{N}_2 + \mathbf{N}_2^{\mathrm{T}}) \end{bmatrix}$$

From Eq. (18), we can see that if

$$\hat{\boldsymbol{\Sigma}} + \bar{\tau}\hat{\boldsymbol{\Gamma}}_1^{\mathrm{T}}\mathbf{R}\hat{\boldsymbol{\Gamma}}_1 < 0 \quad \text{and} \quad \boldsymbol{\Psi} > 0 \tag{19}$$

is satisfied, $\dot{V} < 0$, so the closed-loop system Eq. (6) is asymptotically stable. Next we prove that the two expressions given in Eq. (19) are satisfied if Eq. (10) holds. Consider the first expression $\hat{\boldsymbol{\Sigma}} + \bar{\tau}\hat{\boldsymbol{\Gamma}}_1^{\mathrm{T}}\mathbf{R}\hat{\boldsymbol{\Gamma}}_1 < 0$ in Eq. (19). Since $\hat{\boldsymbol{\Sigma}} + \bar{\tau}\hat{\boldsymbol{\Gamma}}_1^{\mathrm{T}}\mathbf{R}\hat{\boldsymbol{\Gamma}}_1 < 0$ and $-\bar{\tau}\mathbf{R}^{-1} < 0$, from the conditions (i) and (iii) of Lemma 1, we can obtain

$$\begin{bmatrix} \bar{\hat{\boldsymbol{\Sigma}}} + \bar{\tau}\mathbf{X} & \bar{\tau}\hat{\boldsymbol{\Gamma}}_1^{\mathrm{T}} \\ * & -\bar{\tau}\mathbf{R}^{-1} \end{bmatrix} < 0 \tag{20}$$

Then consider the second expression $\boldsymbol{\Psi} > 0$ in Eq. (19). Let $\hat{\boldsymbol{\Gamma}}_2 = [\mathbf{N}_1^{\mathrm{T}} \quad \mathbf{N}_2^{\mathrm{T}}]$, the expression of $\boldsymbol{\Psi}$ under Eq. (17) can be changed to be $\boldsymbol{\Psi} = \begin{bmatrix} \mathbf{X} & \hat{\boldsymbol{\Gamma}}_2^{\mathrm{T}} \\ * & \mathbf{R} \end{bmatrix}$, by multiplying $(-\bar{\tau})$, we have

$$\begin{bmatrix} -\bar{\tau}\mathbf{X} & -\bar{\tau}\hat{\boldsymbol{\Gamma}}_2^{\mathrm{T}} \\ * & -\bar{\tau}\mathbf{R} \end{bmatrix} < 0 \tag{21}$$

Applying the conditions (i) and (iii) of Lemma 1, from Eq. (21) we can obtain

$$-\bar{\tau}\mathbf{X} - (-\bar{\tau})\hat{\boldsymbol{\Gamma}}_2^{\mathrm{T}} \times \left(-\frac{1}{\bar{\tau}}\right)\mathbf{R}^{-1} \times (-\bar{\tau})\hat{\boldsymbol{\Gamma}}_2^{\mathrm{T}} = -\bar{\tau}\mathbf{X} - \bar{\tau}\hat{\boldsymbol{\Gamma}}_2^{\mathrm{T}} \times \left(-\frac{1}{\bar{\tau}}\right)\mathbf{R}^{-1} \times \bar{\tau}\hat{\boldsymbol{\Gamma}}_2^{\mathrm{T}} < 0 \tag{22}$$

By using Lemma 1, from Eq. (22) and $-\bar{\tau}\mathbf{R} < 0$ we can obtain

$$\begin{bmatrix} -\bar{\tau}\mathbf{X} & \bar{\tau}\hat{\boldsymbol{\Gamma}}_2^{\mathrm{T}} \\ * & -\bar{\tau}\mathbf{R} \end{bmatrix} < 0 \tag{23}$$

Applying Lemma 2 for Eqs (20) and (23) leads to

$$\begin{bmatrix} \bar{\hat{\boldsymbol{\Sigma}}} & \bar{\tau}\hat{\boldsymbol{\Gamma}}_1^{\mathrm{T}} & \bar{\tau}\hat{\boldsymbol{\Gamma}}_2^{\mathrm{T}} \\ * & -\bar{\tau}\mathbf{R}^{-1} & \mathbf{0} \\ * & * & -\bar{\tau}\mathbf{R} \end{bmatrix} < 0 \tag{24}$$

So Eq. (19) is satisfied if Eq. (24) holds.
Substituting the expressions of $\bar{\hat{\boldsymbol{\Sigma}}}$, $\hat{\boldsymbol{\Gamma}}_1$ and $\hat{\boldsymbol{\Gamma}}_2$ into Eq. (24) yields

$$\begin{bmatrix} \mathbf{A}^{\mathrm{T}}\mathbf{P} + \mathbf{P}\mathbf{A} + \mathbf{Q} + \mathbf{N}_1 + \mathbf{N}_1^{\mathrm{T}} & \mathbf{P}\mathbf{B}_K - \mathbf{N}_1 + \mathbf{N}_2^{\mathrm{T}} & \bar{\tau}\mathbf{A}^{\mathrm{T}} & \bar{\tau}\mathbf{N}_1 \\ * & -\mathbf{Q} - \mathbf{N}_2 - \mathbf{N}_2^{\mathrm{T}} & \bar{\tau}\mathbf{B}_K^{\mathrm{T}} & \bar{\tau}\mathbf{N}_2 \\ * & * & -\bar{\tau}\mathbf{R}^{-1} & \mathbf{0} \\ * & * & * & -\bar{\tau}\mathbf{R} \end{bmatrix} < 0 \tag{25}$$

Equation (25) can be rewritten as

$$\begin{bmatrix} \boldsymbol{\Xi}_{11} & \boldsymbol{\Xi}_{12} & \bar{\tau}\mathbf{A}^{\mathrm{T}} & \bar{\tau}\mathbf{N}_1 \\ * & \boldsymbol{\Xi}_{22} & \bar{\tau}\mathbf{B}_K^{\mathrm{T}} & \bar{\tau}\mathbf{N}_2 \\ * & * & -\bar{\tau}\mathbf{R}^{-1} & \mathbf{0} \\ * & * & * & -\bar{\tau}\mathbf{R} \end{bmatrix} < 0 \tag{26}$$

Comparing Eq. (10) with Eq. (26), it is easy to see that Eq. (10) becomes Eq. (26) if the third and sixth columns, and the third and sixth rows in Eq. (10) are deleted. From Ref. [27], we know that, when Eq. (10) holds, Eq. (26) will holds too, so the close-loop system Eq. (6) is asymptotic stable when the delay τ is within $0 \leqslant \tau \leqslant \bar{\tau}$.

Then we will prove that under zero initial conditions, $\|\mathbf{z}(t)\|_2 < \gamma\|\mathbf{w}(t)\|_2$ holds for any nonzero $\mathbf{w}(t) \in L_2[0, +\infty)$.

Adding $\mathbf{z}^{\mathrm{T}}(t)\mathbf{z}(t) - \gamma^2\mathbf{w}^{\mathrm{T}}(t)\mathbf{w}(t)$ to both side of Eq. (17) and rearranging the expression, we have

$$\dot{V} + \mathbf{z}^{\mathrm{T}}(t)\mathbf{z}(t) - \gamma^2\mathbf{w}^{\mathrm{T}}(t)w(t) \leqslant \boldsymbol{\eta}_2^{\mathrm{T}}(t)(\boldsymbol{\Sigma} + \bar{\tau}\boldsymbol{\Gamma}_1^{\mathrm{T}}\mathbf{R}\boldsymbol{\Gamma}_1 + \boldsymbol{\Gamma}_3^{\mathrm{T}}\boldsymbol{\Gamma}_3)\boldsymbol{\eta}_2(t) - \int_{t-\tau}^{t} \boldsymbol{\eta}_3^{\mathrm{T}}(t,s)\boldsymbol{\Psi}\boldsymbol{\eta}_3(t,s)\mathrm{d}s \quad (27)$$

where $\boldsymbol{\Gamma}_2 = [\mathbf{C}_1 \quad \mathbf{D}_K \quad \mathbf{D}_{11}]$.

From Eq. (27), we know that if

$$\boldsymbol{\Sigma} + \bar{\tau}\boldsymbol{\Gamma}_1^{\mathrm{T}}\mathbf{R}\boldsymbol{\Gamma}_1 + \boldsymbol{\Gamma}_2^{\mathrm{T}}\boldsymbol{\Gamma}_2 < 0 \quad \text{and} \quad \boldsymbol{\Psi} > 0 \quad (28)$$

are satisfied, then

$$\dot{V} + \mathbf{z}^{\mathrm{T}}(t)\mathbf{z}(t) - \gamma^2\mathbf{w}^{\mathrm{T}}(t)\mathbf{w}(t) < 0 \quad (29)$$

For this, we need to prove Eq. (28) being satisfied when Eq. (10) holds. This prove process is similar to that for Eq. (19). That is, applying Lemma 2 for $(-\bar{\tau})\boldsymbol{\Psi} < 0$ and $\boldsymbol{\Sigma} + \bar{\tau}\boldsymbol{\Gamma}_1^{\mathrm{T}}\mathbf{R}\boldsymbol{\Gamma}_1 + \boldsymbol{\Gamma}_2^{\mathrm{T}}\boldsymbol{\Gamma}_2 < 0$, we can obtain

$$\begin{bmatrix} \bar{\boldsymbol{\Sigma}} & \bar{\tau}\boldsymbol{\Gamma}_1^{\mathrm{T}} & \bar{\tau}\boldsymbol{\Gamma}_3^{\mathrm{T}} & \boldsymbol{\Gamma}_2^{\mathrm{T}} \\ * & -\bar{\tau}\mathbf{R}^{-1} & \mathbf{0} & \mathbf{0} \\ * & * & -\bar{\tau}\mathbf{R} & \mathbf{0} \\ * & * & * & -\mathbf{I} \end{bmatrix} < 0 \quad (30)$$

where

$$\bar{\boldsymbol{\Sigma}} = \begin{bmatrix} \boldsymbol{\Xi}_{11} & \boldsymbol{\Xi}_{12} & \mathbf{P}\mathbf{B}_1 \\ * & \boldsymbol{\Xi}_{22} & \mathbf{0} \\ * & * & -\gamma^2\mathbf{I} \end{bmatrix}, \quad \boldsymbol{\Gamma}_3 = [\mathbf{N}_1^{\mathrm{T}} \quad \mathbf{N}_1^{\mathrm{T}} \quad \mathbf{0}]$$

It is easy to see that Eq. (10) is the same matrix inequality as Eq. (30). Therefore, Eq. (30) is satisfied if Eq. (10) holds, thus Eq. (29) can be obtained.

Integrating Eq. (29) from 0 to ∞ yields

$$\int_0^\infty [\mathbf{z}^{\mathrm{T}}(t)\mathbf{z}(t) - \gamma^2\mathbf{w}^{\mathrm{T}}(t)\mathbf{w}(t)]\mathrm{d}t < V(0) - V(\infty) \quad (31)$$

Since $V(t, \mathbf{x}_t)|_{t=0} = 0$ and $V(t, \mathbf{x}_t)|_{t=\infty} = 0$, so

$$\int_0^\infty [\mathbf{z}^{\mathrm{T}}(t)\mathbf{z}(t) - \gamma^2\mathbf{w}^{\mathrm{T}}(t)\mathbf{w}(t)]\mathrm{d}t < 0 \quad (32)$$

i.e.,

$$\|\mathbf{z}(t)\|_2 < \gamma\|\mathbf{w}(t)\|_2 \quad (33)$$

Therefore, Eq. (10) implies that for any nonzero $\mathbf{w}(t) \in L_2[0, +\infty)$, there holds $\|\mathbf{z}(t)_2\| < \gamma\|\mathbf{w}(t)\|_2$ under zero initial conditions with H_∞ performance index γ. This completes the proof.

3.2. H_∞ controller

The inequality Eq. (10) is a nonlinear matrix inequality, which cannot be solved directly using the LMI Toolbox in MATLAB. In this section, the parameter adjustment method given in [3,5] is used to handle Eq. (10) by introducing two adjustable parameters λ and ρ. When λ and ρ are given and $\bar{\tau}$ is known, Eq. (10) will becomes a linear matrix inequality (LMI), so the LMI Toolbox can be used to obtain H_∞ controller.

Define

$$\mathbf{W} = \begin{bmatrix} \mathbf{P} & \mathbf{0} \\ \mathbf{N}_1^{\mathrm{T}} & \mathbf{N}_2^{\mathrm{T}} \end{bmatrix}, \quad \bar{\mathbf{A}} = \begin{bmatrix} \mathbf{A} & \mathbf{B}_K \\ \mathbf{I} & -\mathbf{I} \end{bmatrix} \tag{34}$$

The following two matrices composed of the elements of the matrix inequality Eq. (10) can be written as

$$\begin{bmatrix} \boldsymbol{\Xi}_{11} & \boldsymbol{\Xi}_{12} \\ * & \boldsymbol{\Xi}_{22} \end{bmatrix} = \mathbf{W}^{\mathrm{T}}\bar{\mathbf{A}} + \bar{\mathbf{A}}^{\mathrm{T}}\mathbf{W} + \begin{bmatrix} \mathbf{Q} & \mathbf{0} \\ \mathbf{0} & -\mathbf{Q} \end{bmatrix} \tag{35}$$

$$\begin{bmatrix} \mathbf{P}\mathbf{B}_1 & \bar{\tau}\mathbf{N}_1 \\ \mathbf{0} & \bar{\tau}\mathbf{N}_2 \end{bmatrix} = \mathbf{W}^{\mathrm{T}} \begin{bmatrix} \mathbf{B}_1 & \mathbf{0} \\ \mathbf{0} & \bar{\tau}\mathbf{I} \end{bmatrix} \tag{36}$$

If $\mathbf{N}_2$ is invertible, $\mathbf{W}$ is nonsingular. Let

$$\mathbf{W}^{-1} = \begin{bmatrix} \mathbf{P}^{-1} & \mathbf{0} \\ \mathbf{M}_1 & \mathbf{M}_2 \end{bmatrix}, \quad \boldsymbol{\chi} = \mathrm{diag}\{\mathbf{W}^{-1}, \mathbf{I}, \mathbf{I}, \mathbf{R}^{-1}, \mathbf{I}, \mathbf{I}\} \tag{37}$$

And using contraction transformation for the matrix $\boldsymbol{\Xi}$ given in Eq. (10), left multiplying $\boldsymbol{\chi}^{\mathrm{T}}$ and right multiplying $\boldsymbol{\chi}$, Eq. (10) becomes

$$\begin{bmatrix} \boldsymbol{\theta}_{11} & \boldsymbol{\theta}_{12} & \mathbf{B}_1 & \boldsymbol{\theta}_{13} & \mathbf{0} & \mathbf{P}^{-1}\mathbf{C}_1^{\mathrm{T}} \\ * & \boldsymbol{\theta}_{22} & \mathbf{0} & \bar{\tau}\mathbf{M}_2^T\mathbf{B}_K^{\mathrm{T}} & \bar{\tau}\mathbf{R}^{-1} & \mathbf{P}^{-1}\mathbf{D}_K^{\mathrm{T}} \\ * & * & -\gamma^2\mathbf{I} & \bar{\tau}\mathbf{B}_1^{\mathrm{T}} & \mathbf{0} & \mathbf{D}_{11}^{\mathrm{T}} \\ * & * & * & -\bar{\tau}\mathbf{R}^{-1} & \mathbf{0} & \mathbf{0} \\ * & * & * & * & -\bar{\tau}\mathbf{R}^{-1} & \mathbf{0} \\ * & * & * & * & * & -\mathbf{I} \end{bmatrix} < 0 \tag{38}$$

where

$$\boldsymbol{\theta}_{11} = \mathbf{P}^{-1}\mathbf{A}^{\mathrm{T}} + \mathbf{A}\mathbf{P}^{-1} + \mathbf{B}_K\mathbf{M}_1 + \mathbf{M}_1^{\mathrm{T}}\mathbf{B}_K^{\mathrm{T}} - \mathbf{M}_1^{\mathrm{T}}\mathbf{Q}\mathbf{M}_1 + \mathbf{P}^{-1}\mathbf{Q}\mathbf{P}^{-1}$$

$$\boldsymbol{\theta}_{12} = \mathbf{P}^{-1} - \mathbf{M}_1^{\mathrm{T}} + \mathbf{B}_K\mathbf{M}_2 - \mathbf{M}_1^{\mathrm{T}}\mathbf{Q}\mathbf{M}_2$$

$$\boldsymbol{\theta}_{22} = -\mathbf{M}_2^{\mathrm{T}}\mathbf{Q}\mathbf{M}_2 - \mathbf{M}_2^{\mathrm{T}} - \mathbf{M}_2$$

$$\boldsymbol{\theta}_{13} = \bar{\tau}(\mathbf{P}^{-1}\mathbf{A}^{\mathrm{T}} + \mathbf{M}_1^{\mathrm{T}}\mathbf{B}_K^{\mathrm{T}})$$

Let $\mathbf{M}_1 = \lambda\mathbf{Q}^{-1}$, $\mathbf{M}_2 = \rho\mathbf{Q}^{-1}$, $\overline{\mathbf{P}} = \mathbf{P}^{-1}$, $\overline{\mathbf{R}} = \mathbf{R}^{-1}$, $\overline{\mathbf{Q}} = \mathbf{Q}^{-1}$ and $\overline{\mathbf{Y}} = \mathbf{K}\mathbf{Q}^{-1}$ where λ and ρ are both real number, $\rho \neq 0$, i.e., $\lambda, \rho \in R, \rho \in R, \rho \neq 0$. Applying Lemma 1, we have the following theorem.

Theorem 2. *Given* , $\overline{\tau} > 0, \lambda \in R, 0 \neq \rho \in R$, *if there exist real matrices*, $\overline{\mathbf{P}} > 0$, $\overline{\mathbf{R}} > 0$, $\overline{\mathbf{Q}} > 0$ *and* $\mathbf{Y}$ *satisfying the matrix inequality*

$$\begin{bmatrix} \boldsymbol{\omega}_{11} & \boldsymbol{\omega}_{12} & \mathbf{B}_1 & \boldsymbol{\omega}_{13} & \mathbf{0} & \bar{\mathbf{P}}\mathbf{C}_1^{\mathrm{T}} & \bar{\mathbf{P}} \\ * & \boldsymbol{\omega}_{22} & \mathbf{0} & \bar{\tau}\rho\mathbf{Y}^{\mathrm{T}}\mathbf{B}_2^{\mathrm{T}} & \bar{\tau}\bar{\mathbf{R}} & \rho\mathbf{Y}^{\mathrm{T}}\mathbf{D}_{12}^{\mathrm{T}} & \mathbf{0} \\ * & * & -\gamma^2\mathbf{I} & \bar{\tau}\mathbf{B}_1^{\mathrm{T}} & \mathbf{0} & \mathbf{D}_{11}^{\mathrm{T}} & \mathbf{0} \\ * & * & * & -\bar{\tau}\bar{\mathbf{R}} & \mathbf{0} & \mathbf{0} & \mathbf{0} \\ * & * & * & * & -\bar{\tau}\bar{\mathbf{R}} & \mathbf{0} & \mathbf{0} \\ * & * & * & * & * & -\mathbf{I} & \mathbf{0} \\ * & * & * & * & * & * & -\bar{\mathbf{Q}} \end{bmatrix} \tag{39}$$

where

$$\boldsymbol{\omega}_{11} = \bar{\mathbf{P}}\mathbf{A}^{\mathrm{T}} + \mathbf{A}\bar{\mathbf{P}} + \lambda\mathbf{B}_2\mathbf{Y} + \lambda\mathbf{Y}^{\mathrm{T}}\mathbf{B}_2^{\mathrm{T}} - \lambda^2\bar{\mathbf{Q}}$$

$$\boldsymbol{\omega}_{12} = \bar{\mathbf{P}} - \lambda\bar{\mathbf{Q}} + \rho\mathbf{B}_2\mathbf{Y} - \lambda\rho\bar{\mathbf{Q}}$$

$$\boldsymbol{\omega}_{22} = -\rho^2\bar{\mathbf{Q}} - 2\rho\bar{\mathbf{Q}}$$

$$\boldsymbol{\omega}_{13} = \bar{\tau}(\bar{\mathbf{P}}\mathbf{A}^{\mathrm{T}} + \lambda\mathbf{Y}^{\mathrm{T}}\mathbf{B}_2^{\mathrm{T}})$$

the closed-loop system Eq. (6) *is asymptotically stable with H_∞ performance index γ for any time delay τ satisfying $0 \leqslant \tau \leqslant \bar{\tau}$, and the H_∞ control feedback gain is $\mathbf{K} = \mathbf{Y}\bar{\mathbf{Q}}^{-1}$.*

4. Three control design problems

4.1. Controller design with known maximum time delay

If $\bar{\tau}$, λ and ρ are all known, Eq. (39) becomes a linear matrix inequality, $\mathbf{K}$ can be obtained by solving this inequality using the MATLAB LMI Toolbox. This controller can guarantee the closed-loop system Eq. (6) being asymptotically stable as long as the real time delay in the system is within $0 \leqslant \tau \leqslant \bar{\tau}$ whether this delay is time-varying or not. Herein we consider the following question: when $\bar{\tau}$ is known, how to select λ and ρ may let $\mathbf{K}$ achieves better control effectiveness. In this paper, the genetic algorithm is used to optimize λ and ρ by minimizing the index γ in the LMI Eq. (39). The detailed process is described as follows.

The genetic algorithm is a probabilistic search procedure based on the mechanism of natural selection and natural genetics. It has been successfully applied to different controller synthesis problems for its high potential in global optimization [19]. In this section, the objective function is described as

$$\min_{\lambda,\rho} \gamma \quad \text{subject to LMI Eq. (39)} \tag{40}$$

When $\bar{\tau}$ is known, the genetic algorithm randomly generates initial λ and ρ which changes thereafter within the evolution procedure according to objective Eq. (40). The detailed technique can be described in the following steps:

Step 1: use the binary string to encode λ and ρ;
Step 2: randomly generate an initial population of N_p chromosomes, $N_p = 200$ is taken in this paper;
Step 3: substituting λ and ρ into Eq. (39) to solve the objective function γ. Decode the initial population produced in Step 2 into real values for λ_j and ρ_j, $j = 1, 2 \cdots N_p$. For every λ_j and ρ_j, solving the LMI Eq. (39) to obtain the objective function γ, and then associate every λ_j and ρ_j with a suitable fitness value according to rank-based fitness assignment approach, and then go to Step 4;
Step 4: use tournament selection approach to choose the offspring;
Step 5: perform uniform crossover with probability p_c to produce new offspring, $p_c = 0.8$ is taken in this paper;
Step 6: do bit mutation in the population of chromosomes with a small mutation probability p_m, in this paper $p_m = 0.02$ is taken;
Step 7: retain the best chromosomes in the population with elitist reinsertion method;
Step 8: the evolution process will repeat for N_g generations or being ended when the search process converges with a given accuracy. Or else go to Step 3. In this paper, $N_g = 500$ is taken.

Finally, the best chromosome is decoded into real λ and ρ, substituting λ, ρ and $\bar{\tau}$ into Eq. (39) to obtain the optimal $\mathbf{K}$.

4.2. Maximum time delay with a known controller

For a control system, the task of control design is to obtain the feedback gain $\mathbf{K}$. The gain $\mathbf{K}$ is different when different control design methods are used. We hope that the controller designed should have strong robustness to the variation of structural intrinsic parameters and external disturbance. As mentioned in the "INTRODUCTION", time delay exists inevitably in active control systems. Therefore, it is worth considering the following question: in what range of time delay the controller $\mathbf{K}$ designed in the case of no time delay is applicable? We certainly expect that this range to be as large as possible. In this section, the genetic algorithm will be used to find the maximum time delay for the case when $\mathbf{K}$ is known.

From Theorems 1 and 2, we know that the stability condition Eq. (10) is equivalent to the matrix inequalities Eq. (39). So for a given $\mathbf{K}$, the time-delay control system Eq. (6) is asymptotically stable if Eq. (39) is satisfied. This paper will determine the maximum time delay by using the following method. Assume that the feedback gain $\mathbf{K}$ has been obtained using a certain control design method. Equation (39) is still nonlinear after the substitution of $\mathbf{K}$ into Eq. (39). Substituting a small delay τ into Eq. (39) and then using the feasp function of LMI Toolbox to verify if Eq. (39) is satisfied. If Eq. (39) holds, increasing τ, and then repeat the above process until Eq. (39) does not hold. In this way, the maximum time delay can be determined.

The above process for determining the maximum time delay also involves the choosing of λ and ρ. Here we also use the genetic algorithm to optimize λ and ρ. Different from that in Section 4.1, the objective function used herein is the maximum time delay $\bar{\tau}$.

The objective function is described as

$$\max_{\lambda,\rho} \bar{\tau} \quad \text{subject to LMI Eq. (39)} \tag{41}$$

The optimization is similar to that in Section 4.1 and omitted herein. The maximum time delay for a known $\mathbf{K}$ can be determined using Eq. (41). However, this method can not guarantee that γ attains minimum. In other words, $\mathbf{K}$ can only guarantee that the closed-loop system Eq. (6) is asymptotically stable for the delay τ satisfying $0 \leqslant \tau \leqslant \bar{\tau}$, but can not guarantee that the control effectiveness is the best. Here we design the best $\mathbf{K}$ using the following treating process: (i) a feedback gain $\mathbf{K}$ is first designed using the classical LQR method; (ii) substituting $\mathbf{K}$ into Eq. (39) to get a maximum time delay $\bar{\tau}$; and (iii) under this $\bar{\tau}$, the best $\mathbf{K}'$ can be obtained using the method in Section 4.1. Experimental results in Section 5 will show that $\mathbf{K}'$ can achieve better control efficiency than $\mathbf{K}$.

4.3. The biggest time delay for system stability with unknown controller

In Section 4.2, the maximum time delay $\bar{\tau}$ corresponding to a known $\mathbf{K}$ is discussed. If $\mathbf{K}$ is unknown, how much will the maximum time delay be? For this case, how to obtain the feedback gain $\mathbf{K}$? These questions are discussed below.

From the above we know that system stability can be verified using the matrix inequality Eq. (39). The system is asymptotically stable if Eq. (39) is satisfied. Here we directly use the optimization problem given by Eq. (39) to determine the maximum time delay, where the objective function is $\bar{\tau}$, constraint condition is the matrix inequality Eq. (39), and the optimezation variables are λ and ρ. The genetic algorithm is the same as that in Section 4.2. After the maximum time delay $\bar{\tau}$ is obtained, the corresponding feedback gain $\overline{\mathbf{K}}$ can be solved using the method in Section 4.1. Since the feedback gain is not specified in advance in the solution of $\bar{\tau}$, this $\bar{\tau}$ is the biggest one of all the maximum time delays.

5. Simulation and experiment

To demonstrate the feasibility and effectiveness of the proposed method, numerical simulation and experiment are carried out in this section. An epoxy resin plate is adopted as structural model. The length, width and thickness of the plate are 800 mm, 400 mm and 2 mm, respectively, as shown in Fig. 2. Material properties of the plate are as follows: Young's elastic modulus is 16.0 GPa, Poisson's ratio is 0.33 and density is 1840 kg/m^3. In the experiment,

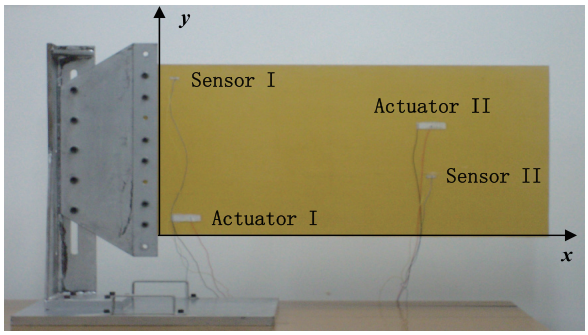

Fig. 2. Photo of experiment plate.

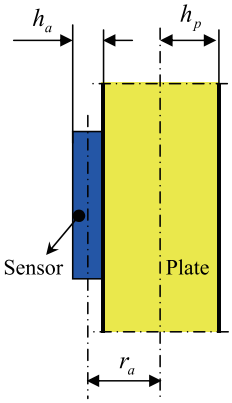

Fig. 3. Sketch map of r_a.

Two PZT patches are used as sensors for measuring the vibration signal of the plate. The other two are used as actuators to control the plate vibration. These two PZT actuators have the same size, given by of 60 mm × 15 mm × 0.5 mm. The size of the two PZT sensors are both to be 20 mm × 5 mm × 0.5 mm. The optimal positions of PZT actuators and sensors are determined using the particle swarm optimizer (PSO) (for details, see Ref. [16]). The coordinate of the middle point of the first PZT actuator (denoted by Actuator I) in the *o-xy* system is (0.06 m, 0.04 m), as shown in Figs 1 and 2. The second PZT actuator (denoted by Actuator II) is at (0.56 m, 0.2595 m). The two PZT sensors are denoted by Sensor I and Sensor II, respectively, and their optimal positions on the plate are (0.06 m, 0.04 m) and (0.56 m, 0.1405 m), respectively. The material parameters of PZT material are as follows: Young's elastic modulus is 63.0 GPa, Poisson's ratio is 0.35, PZT strain constants are $d_{31} = 1.75 \times 10^{-10}$ m/V, PZT stress constant is $e_{31} = 6.98$ N/(V · m). The first two natural frequencies of plate determined by theoretical model are 1.5283 and 6.5843, respectively; the first two natural frequencies determined by experiment are 1.5314 and 6.6291, respectively. In the simulation and experiment, the data sampling period is chosen to be 0.001 s.

With the initial velocity of zero, apply an external force on the bottom-right point of the plate to produce a static displacement of 0.01 m. When releasing the external force, the plate starts a free vibration. The PZT actuators are used to control the plate vibration. Since the free vibration of the plate is mainly dominated by its low-order modes, the following two control cases are considered: (i) only Actuator 1 is used for controlling the plate vibration and Sensor 1 is used as sensor; (ii) Actuators I and II are used for the plate, and Sensors 1 and 2 are used as sensors.

The voltage signal of PZT sensor can be written as [24]

$$V_{sk} = K_{evk} e_{31} r_a \times \left[\int_{y_{s1k}}^{y_{s2k}} \int_{x_{s1k}}^{x_{s2k}} \frac{\partial w^2(x,y,t)}{\partial x^2} \mathrm{d}x\mathrm{d}y + \int_{x_{s1k}}^{x_{s2k}} \int_{y_{s1k}}^{y_{s2k}} \frac{\partial w^2(x,y,t)}{\partial y^2} \mathrm{d}y\mathrm{d}x \right] \tag{42}$$

where K_{evk} is the charge amplifier constant, given by $K_{ev1} = 0.33 \times 10^8$ V/C and $K_{ev2} = 1.67 \times 10^9$ V/C in this paper; r_a is the distance between the middle plane of plate and that of the j-th sensor, as shown in Fig. 3, i.e, $r_a = h_p + 0.5h_a$, where h_p is the half thickness of the plate; (x_{s1k}, y_{s1k}) and (x_{s2k}, y_{s2k}) are the down-left and top-right coordinates of the PZT sensors in the *o-xy* system, k = 1–2, as shown in Fig. 1.

Considering that the transverse displacement $w(x,y,t)$ can be expressed as a time-dependent weighted sum of assumed spatial mode shape functions, given by

$$w(x,y,t) = \sum_{j=1}^{\infty} W_j(x,y)\phi_j(t) \tag{43}$$

where W_j and ϕ_j represent the modal function and modal coordinate of the j-th mode of plate, respectively.

Using Eq. (43), Eq. (42) becomes

$$V_{sk} = b_k \left(\sum_{j=1}^{\infty} \left\langle \int_{y_{s1k}}^{y_{s2k}} [W_{jx}(x_{s2k}, y) - W_{jx}(x_{s1k}, y)] \mathrm{d}y \right.\right.$$

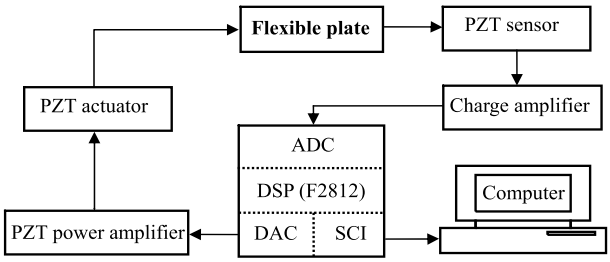

Fig. 4. Flow chart of experiment system.

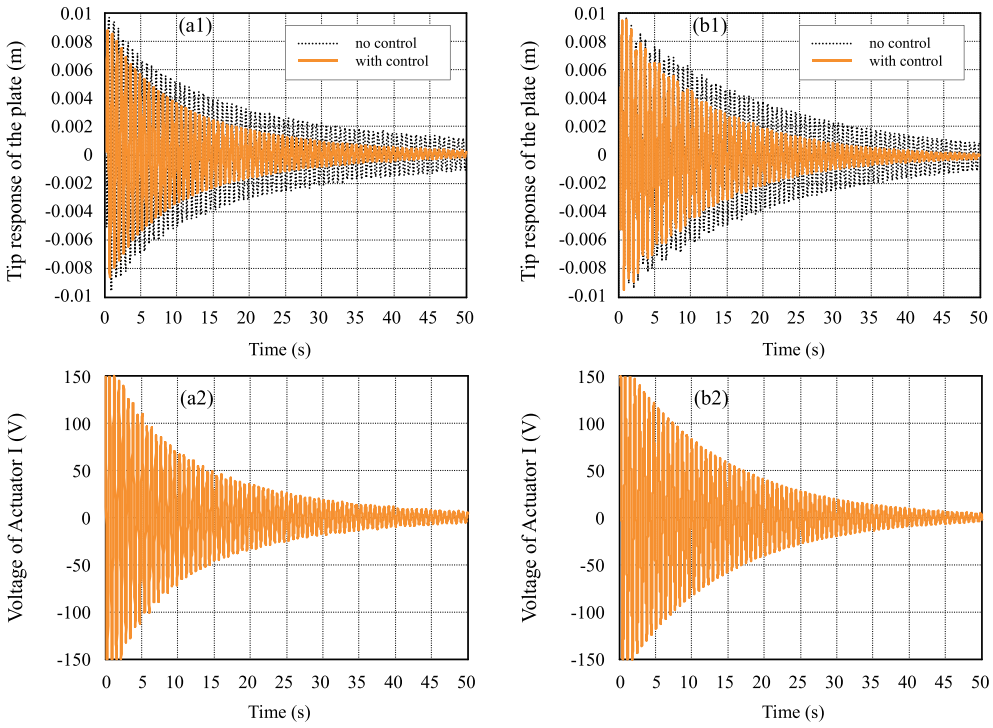

Fig. 5. Response of the plate and applied voltage of Actuator I when $K = [1.4542, 35.0246]$ is used for the plate with time delay $\tau = 0.06$s (one actuator case): (a) experimental result and (b) simulation result.

$$+ \int_{x_{s1k}}^{x_{s2k}} [W_{jy}(x, y_{s2k}) - W_{jy}(x, y_{s1k})]\mathrm{d}x \Big\rangle \phi_j(t) \Big) \tag{44}$$

where $b_k = K_{evk} e_{31} r_a$.

The experiment system is structured based on the DSP TMS320F2812. The flow chart of experiment system is shown in Fig. 4 and the detailed signal flow and process are as follows:

(1) Feedback signal loop: the charge signal produced by the PZT sensors is amplified by the charge amplifier and then enters the ADC module in DSP.
(2) Control signal loop: the voltage signal goes through the two channels of DAC module into the PZT power amplifier where it gets amplified and then it goes into the PZT actuators.
(3) The DSP communicates with the peripheral computer via the SCI module which transfers experimental data to the computer to save and to render diagrams.

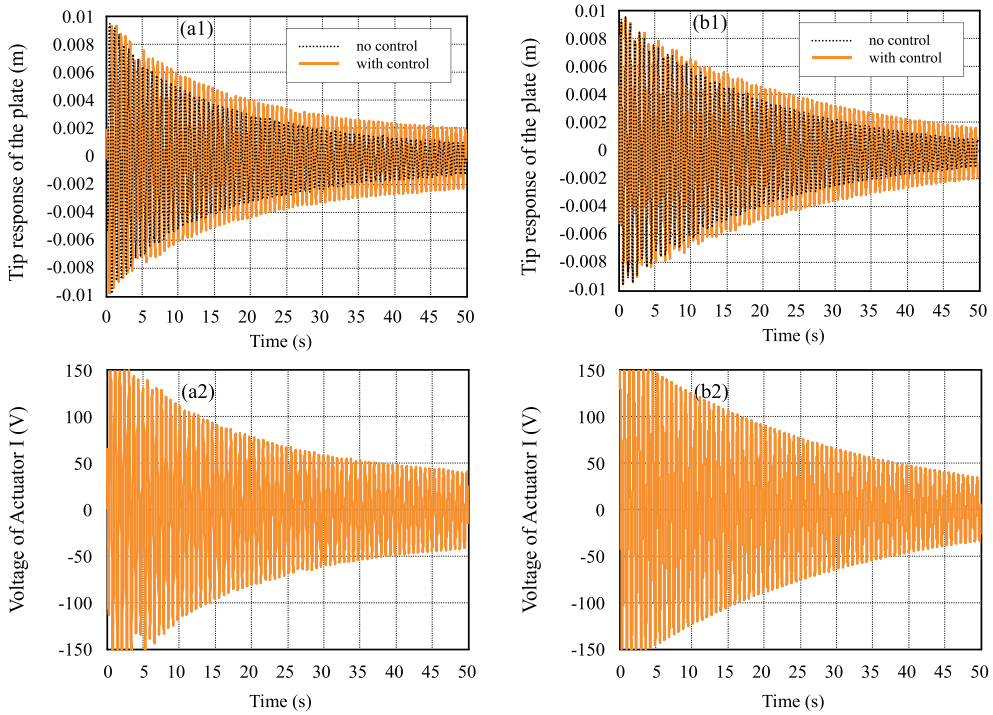

Fig. 6. Response of the plate and applied voltage of Actuator I when $K = [1.4542, 35.0246]$ is used for the plate with time delay (one actuator case): (a) experimental result ($\tau = 0.08$ s), (b) simulation result ($\tau = 0.09$ s).

5.1. Maximum time delay with known controller

Here we consider the determining the maximum time delay of the system when the controller is known. The controller is designed using the classical LQR method. When the feedback gain is obtained, the corresponding maximum stable delay can be determined using the proposed method given in Section 4.2. In Ref. [19], Du and Zhang ever studied H_∞ controller for buildings with time delay in control by linear matrix inequality, and the maximum time delay was investigated using the genetic algorithm. The optimization problem adopted in [19] is the same as Eq. (41), but the linear matrix inequality used in [19] is different from Eq. (41). In this paper, the result using the method given in [19] will be compared with that using the proposed method in Section 4.2.

Firstly, consider the case that Actuator I and Sensor I are used for the plate. When using the LQR method, the gain matrices are chosen as $\hat{\mathbf{Q}} = \mathrm{diag}(100, 1)$ and $\hat{R} = 0.0004$, so the control feedback gain matrix can be determined to be $\mathbf{K} = [1.4542, 35.0246]$. Using the method in Section 4.2, the maximum time delay corresponding to this gain matrix can be determined to be $\bar{\tau} = 0.0852$s, i.e., $\mathbf{K} = [1.4542, 35.0246]$ is available for vibration control of the plate when the real delay in the system is within $0 \leqslant \tau \leqslant 0.0852$ s. Using the method given in Ref. [19], it is $\bar{\tau} = 0.0577$ s, and namely the stability range of time delay is $0 \leqslant \tau \leqslant 0.0577$ s. Assuming the real time delay in the control system is $\tau = 0.06$ s, Fig. 5 shows the simulation and experimental results of the responses of the bottom-right point of the plate and the applied voltages of Actuator I when $\mathbf{K} = [1.4542, 35.0246]$ is applied onto the plate. From Fig. 5 we can observe that the plate vibration can be suppressed effectively, and the experimental results agree better with the simulation ones. Although the real delay $\tau = 0.06$ s is larger than $\bar{\tau} = 0.0577$ s, the control system is still stable. This indicates that the given method in [19] is somewhat conservative. Figure 6 shows the results when the real delays $\tau = 0.08$ s (for the experiment) and $\tau = 0.09$ s (for the simulation) exist in the system, respectively. It is observed from Fig. 6 that the control effectiveness becomes worse when the delayed time is close to or beyond the maximum time delay, since the results with control are larger than those without control. From Figs 5 and 6, we can observe that the maximum time delay determined using the proposed method in this paper is closer to the real one. Although the disabled delays in the experiment are 0.08 s and 0.09 s in numerical simulation, they are not

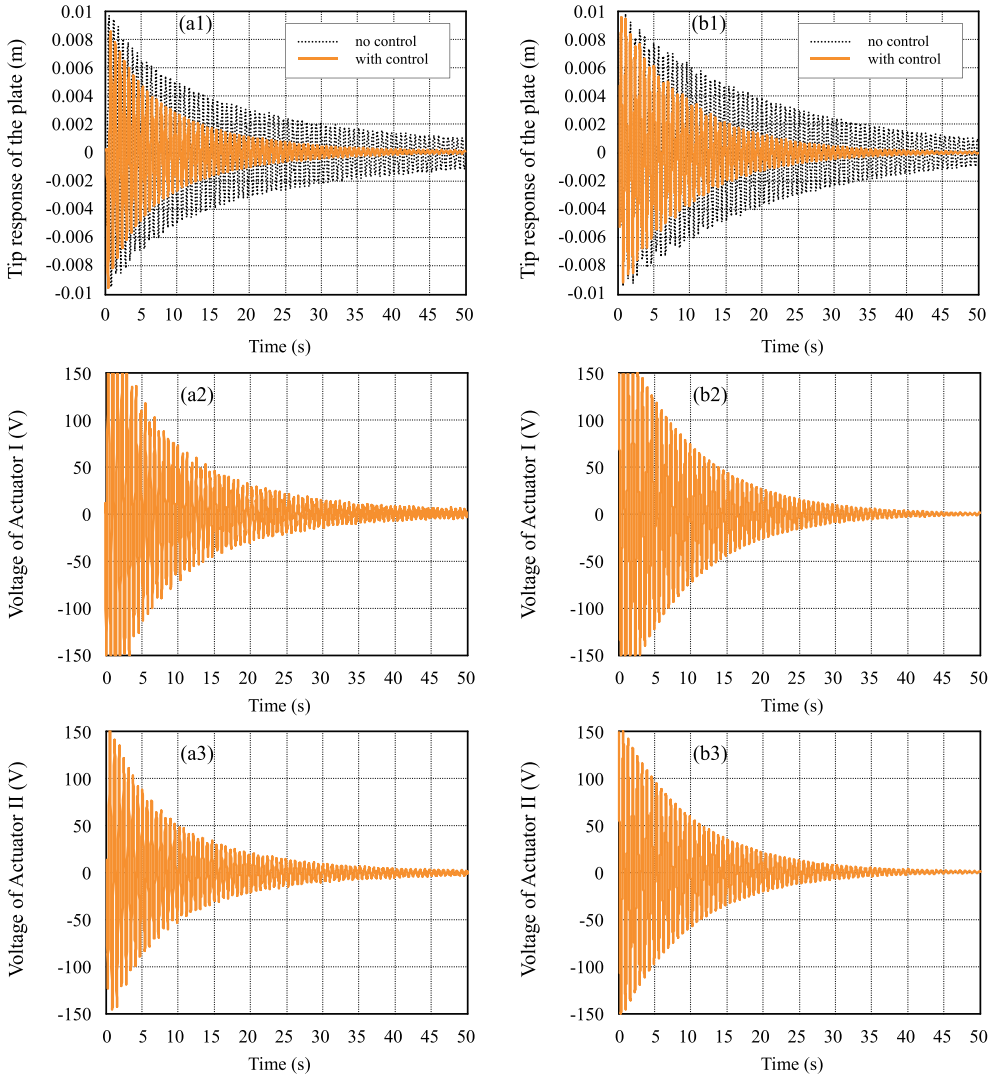

Fig. 7. Response of the plate and applied voltages of the two actuators when $K = \begin{bmatrix} -0.0906 & 22.2168 & -25.7007 & -29.2862 \\ 0.2295 & 11.9850 & -5.4872 & -15.0261 \end{bmatrix}$ is used for the plate with time delays $\tau_1 = \tau_2 = 0.025$s (two actuators case): (a) experimental result, (b) simulation result.

very different. The difference is probably caused by the modeling error and mechanical-electrical disturbance in the experiment.

Then consider that the two actuators and two sensors are all used for the plate. When using the LQR, the gain matrices are chosen as $\hat{\mathbf{Q}} = \mathrm{diag}(100, 100, 1, 1)$ and $\hat{\mathbf{R}} = 10^{-4} \times \mathrm{diag}(6, 3)$, the control feedback gain is

$$\mathbf{K} = \begin{bmatrix} -0.0906 & 22.2168 & -25.7007 & -29.2862 \\ 0.2295 & 11.9850 & -5.4872 & -15.0261 \end{bmatrix}$$

Corresponding to this controller, the maximum time delay is $\bar{\tau} = 0.0369$ s when using the determining method in this paper, and $\bar{\tau} = 0.0203$ s when using the method in Ref. [19]. Figure 7 shows the responses of the bottom-right point of the plate and the applied voltages of PZT actuators when ($\tau_1 = 0.025$ s, $\tau_2 = 0.025$ s) exist in the control system, where τ_1 is the delay in Actuator I and τ_2 in Actuator II. From Fig. 7 we can observe that the plate vibration can be suppressed effectively and the experimental results agree better with the simulation ones. Figure 8 shows the results when the real delays are ($\tau_1 = 0.035$ s, $\tau_2 = 0.035$ s) (for the experiment) and ($\tau_1 = 0.04$ s, $\tau_2 = 0.04$ s)

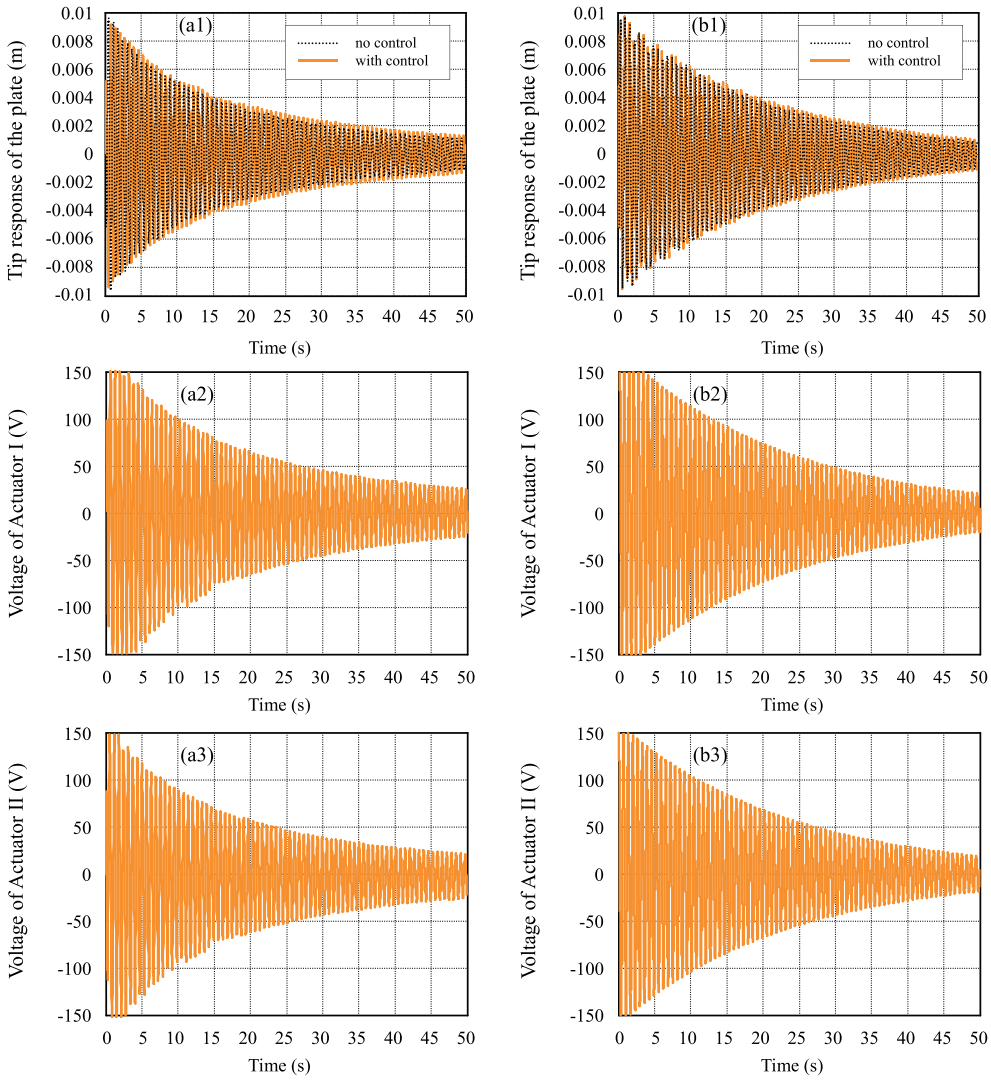

Fig. 8. Response of the plate and applied voltages of the two actuators when $K = \begin{bmatrix} -0.0906 & 22.2168 & -25.7007 & -29.2862 \\ 0.2295 & 11.9850 & -5.4872 & -15.0261 \end{bmatrix}$ is used for the plate with time delays (two actuators case). (a) experimental result ($\tau_1 = \tau_2 = 0.035$s); (b) simulation result ($\tau_1 = \tau_2 = 0.04$s).

(for the simulation), respectively. From Fig. 8 we can observe that the control effectiveness becomes worse when the delayed time is close to or exceed the maximum time delay. The maximum delay determined using the proposed method in this paper is more accurate.

5.2. *Controller design with known maximum time delay*

Here we verify the proposed method in Section 4.1. The control feedback gain $\mathbf{K}$ is first designed using the LQR, and then the best control feedback gain $\mathbf{K}'$ is determined through optimizing λ and ρ by minimizing γ. For simplification of expression, Actuator I and Sensor I are only considered to be used for the plate. The control feedback gain $\mathbf{K}$ is shown in Section 5.1, given by $\mathbf{K} = [1.4542, 35.0246]$, and the corresponding maximum stable delay is $\bar{\tau} = 0.0852$ s. By using the method in Section 4.1, the best controller can be determined to be $\mathbf{K}' = [-49.2654, 62.1756]$. Using $\mathbf{K}$ and $\mathbf{K}'$ for the plate, Fig. 9 shows the experimental results when the real delay $\tau = 0.06$ s exists in the control system. It is observed from Fig. 9 that the control effectiveness using $\mathbf{K}'$ is better

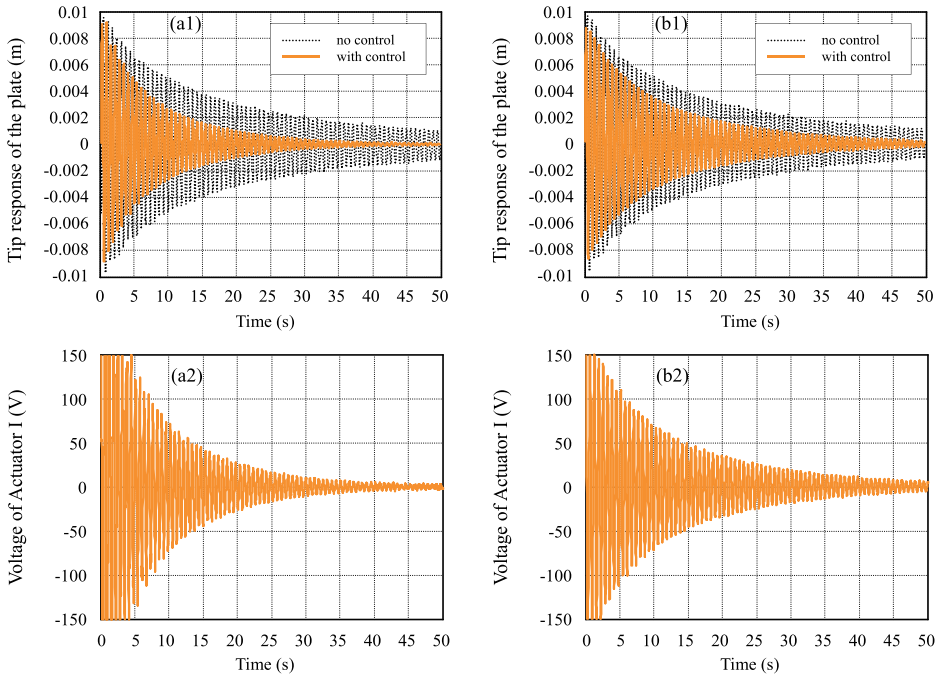

Fig. 9. Response of the plate and applied voltage of Actuator I when $K = [1.4542, 35.0246]$ and $K' = [-49.2654, 62.1756]$ are used for the plate with time delay $\tau = 0.06$s, respectively (one actuator case). (a) experimental result ($K' = [-49.2654, 62.1756]$); (b) experimental result ($K = [1.4542, 35.0246]$).

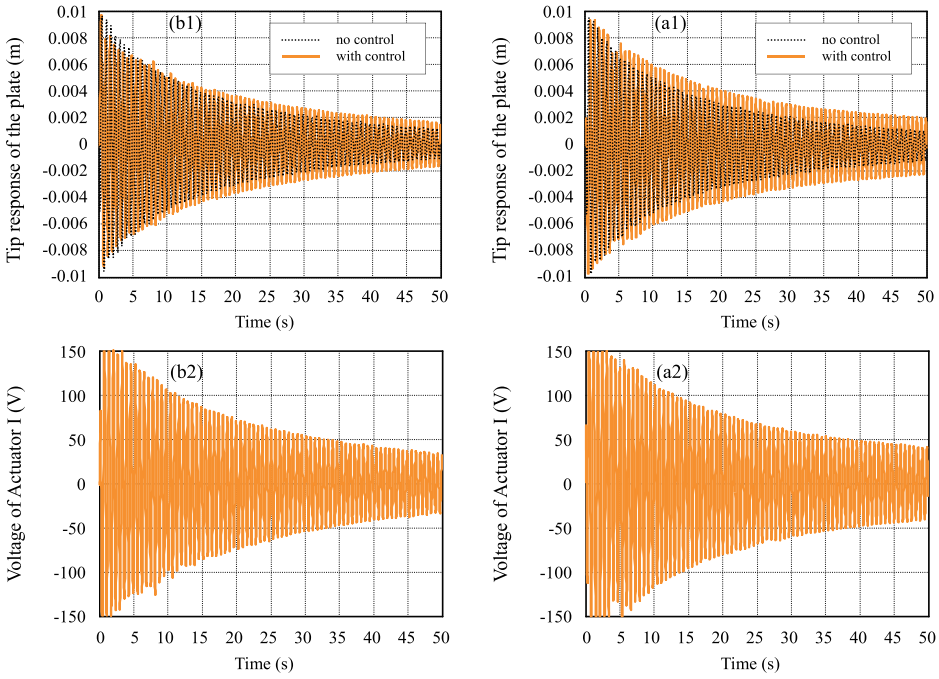

Fig. 10. Response of the plate and applied voltage of Actuator I when $K = [1.4542, 35.0246]$ and $K' = [-49.2654, 62.1756]$ are used for the plate with time delay $\tau = 0.09$s, respectively (one actuator case). (a) experimental result ($K' = [-49.2654, 62.1756]$); (b) experimental result ($K = [1.4542, 35.0246]$).

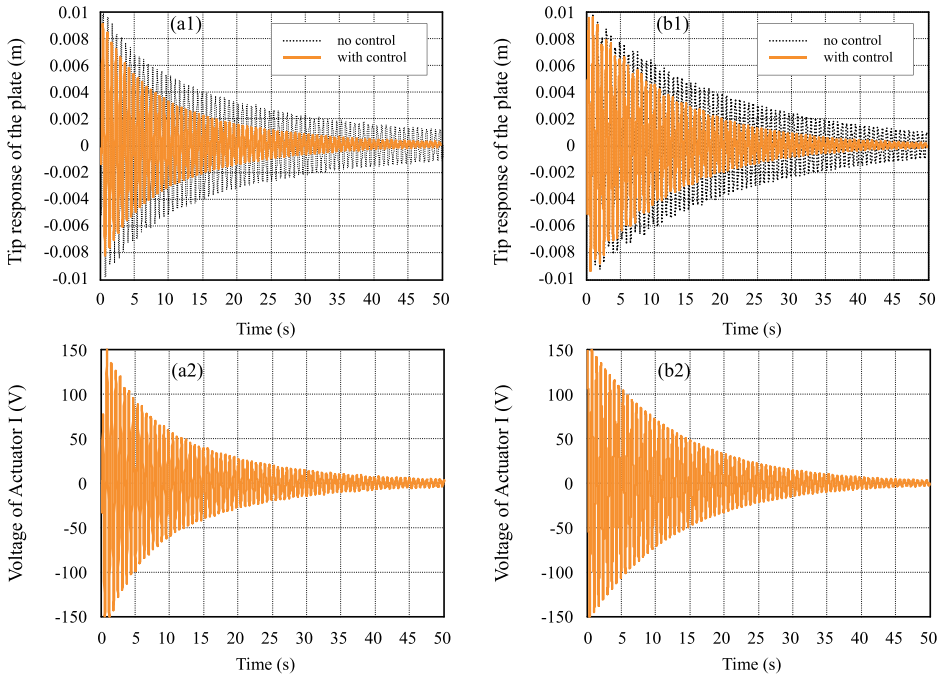

Fig. 11. Response of the plate and applied voltage of Actuator I when $\bar{K} = [-452.2514, 46.1893]$ is used for the plate with time delay $\tau = 0.13$s (one actuator case). (a) experimental result; (b) simulation result.

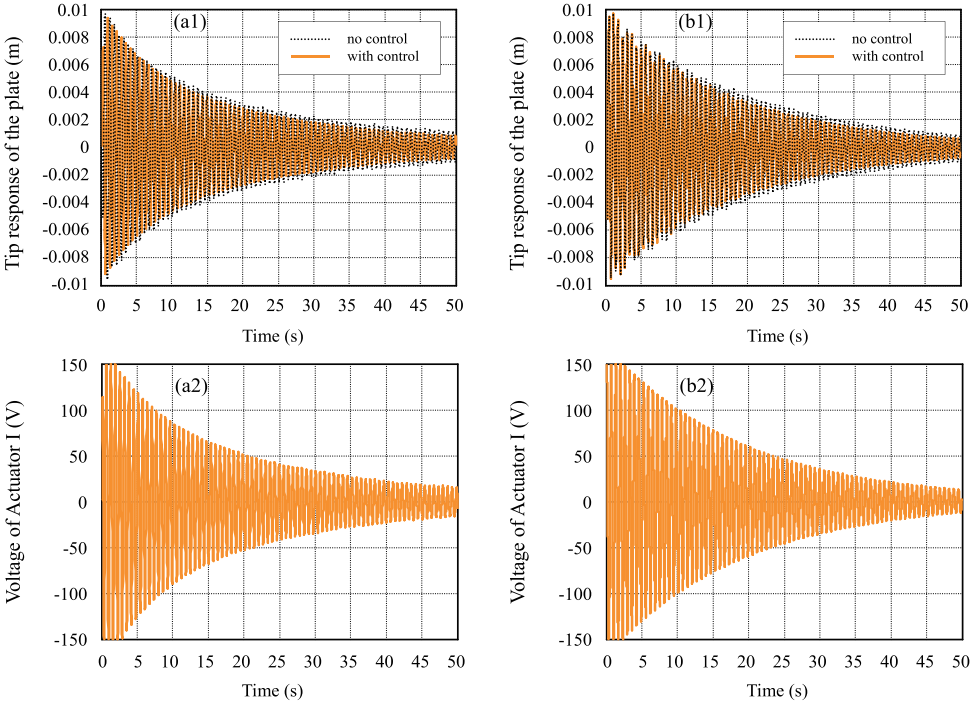

Fig. 12. Response of the plate and applied voltage of Actuator I when $\bar{K} = [-452.2514, 46.1893]$ is used for the plate with time delay $\tau = 0.17$ s (one actuator case). (a) experimental result; (b) simulation result.

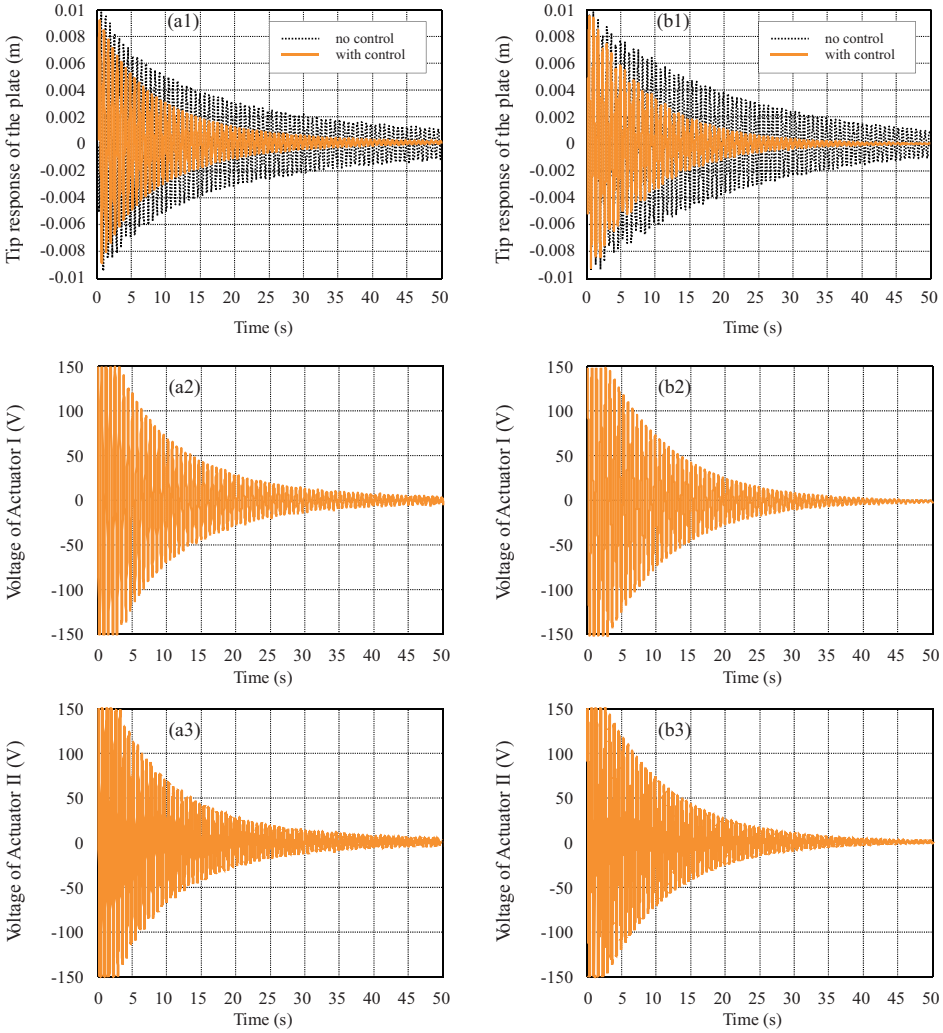

Fig. 13. Response of the plate and applied voltages of the two actuators when $\bar{K} = \begin{bmatrix} 2.3975 & -0.3192 & 24.1597 & 15.0636 \\ 2.3560 & 0.5548 & 18.8113 & 28.1712 \end{bmatrix}$ is used for the plate with time delays ($\tau_1 = 0.04$s, $\tau_2 = 0.06$s) (two actuators case). (a) experimental result; (b) simulation result.

than that using $\mathbf{K}$. Figure 10 shows the results when the real delay is $\tau = 0.09$ s that is larger than $\bar{\tau} = 0.0852$ s. We can observe from Fig. 10 that the control effectiveness becomes worse using both $\mathbf{K}'$ and $\mathbf{K}$ since the results with control are larger than those with no control. The above results demonstrate the validity of the proposed method in Section 4.1.

5.3. The biggest time delay and H_∞ controller

Here we check the validity of the proposed method in Section 4.3. For this case, the controller is unknown in advance. The biggest time delay for stability is solved at first using the optimization algorithm and then H_∞ controller is determined using the method in Section 4.1. Firstly, Actuator I and Sensor I are used for the plate. Using the objective function Eq. (41), the adjusting parameters are $\lambda = 0.51$ and $\rho = 5.72$, so the biggest delay and the corresponding feedback gain can be determined to be $\bar{\tau} = 0.1672$ s and $\bar{\mathbf{K}} = [-452.2514, 46.1893]$, respectively. Figure 11 shows the responses of the bottom-right point of the plate and the applied voltages of Actuator I. It can be seen that when the real delay $\tau = 0.13$ s exists in the control system, the plate vibration can be suppressed effectively.

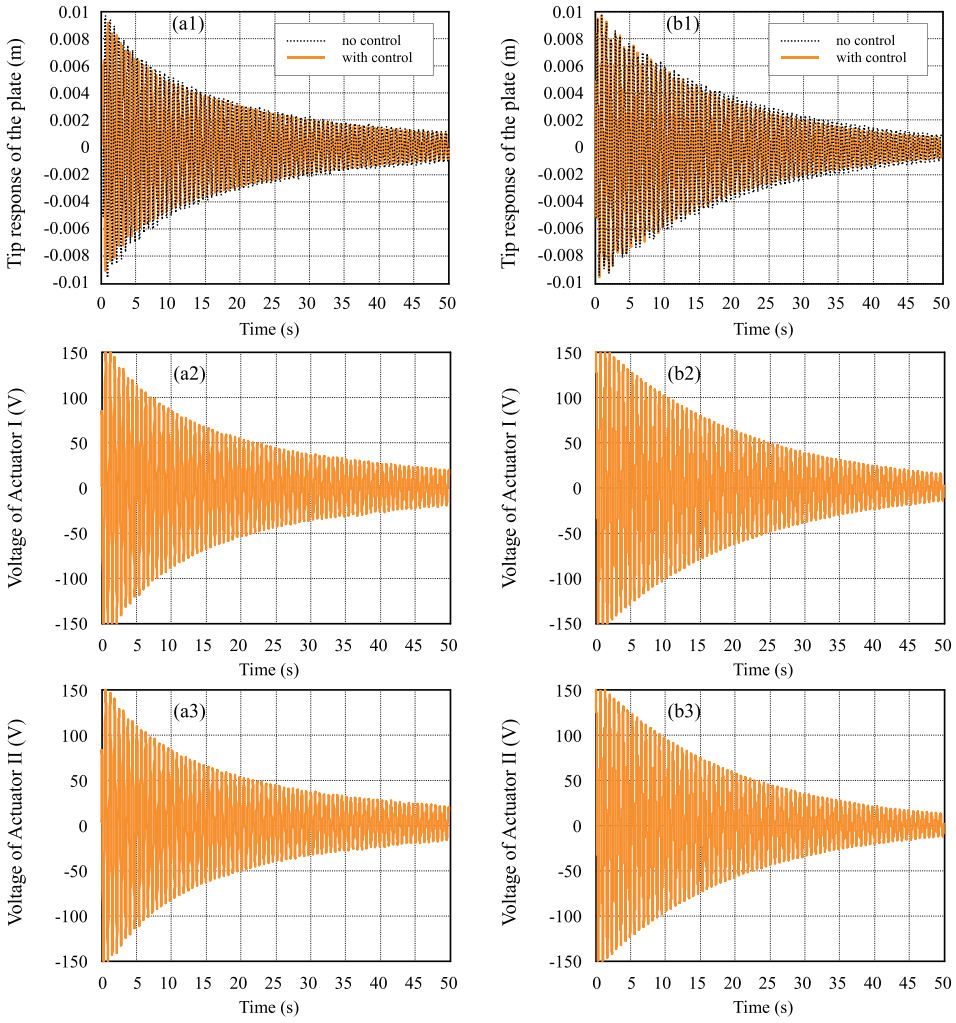

Fig. 14. Response of the plate and applied voltages of the two actuators when $\bar{K} = \begin{bmatrix} 2.3975 & -0.3192 & 24.1597 & 15.0636 \\ 2.3560 & 0.5548 & 18.8113 & 28.1712 \end{bmatrix}$ is used for the plate with time delays (two actuator case). (a) experimental result ($\tau_1 = \tau_2 = 0.07$s); (b) simulation result ($\tau_1 = \tau_2 = 0.08$s).

Figure 12 shows that, when the real delay $\tau = 0.17$ s is larger than $\bar{\tau} = 0.1672$ s, the control effectiveness becomes worse.

Then the two actuators and sensors are all used for the plate. The adjusting parameters are $\lambda = 0.17$ and $\rho = 1.68$, the biggest delay is $\bar{\tau} = 0.0753$ s and the corresponding feedback gain is

$$\bar{\mathbf{K}} = \begin{bmatrix} 2.3975 & -0.3192 & 24.1597 & 15.0636 \\ 2.3560 & 0.5548 & 18.8113 & 28.1712 \end{bmatrix}$$

Figure 13 shows the results when the real delays are ($\tau_1 = 0.04$ s, $\tau_2 = 0.06$ s), the plate vibration is suppressed effectively. Figure 14 shows the results when the real time delays are close to or beyond 0.0753 s, the control effectiveness becomes worse.

6. Conclusions

In this paper, time-delay H_∞ control is numerically and experimentally studied using a flexible plate as research object. A matrix inequality is proposed for stability analysis of the system and a H_∞ controller is designed based on

this matrix inequality. Simulation and experimental results indicate that the proposed controller is applicable for controlling the plate vibration. The maximum time delay determined using the proposed method is more approximate to the real value.

Acknowledgments

This work was supported by the Key Project [grant number 11132001] and the General Projects [grant numbers 11072146, 11002087, 11272202] of Natural Science Foundation of China, and the Specialized Research Fund for the Doctoral Program of Higher Education of China [grant number 20110073110008].

References

[1] J. Mohammad, *Robust Control Systems with Genetic Algorithms*, *CRC Press*, 2002.
[2] M.S. Mahmoud, *Robust Control and Filtering for Time-Delay Systems*, Marcel Dekker, New York, 2000.
[3] M. Wu and Y. He, *Robust Control for Time Delay Systems-Free-Weighting Matrices*, Science Press, Beijing, 2008 (in Chinese).
[4] Y.M. Jia, Robust H_∞ *Control*, Science Press, Beijing, 2007 (in Chinese).
[5] E. Fridman and U. Shaked, Delay-dependent stability and H_∞ control: Constant and time-varying delays, *International Journal of Control* **76**(1) (2003), 48–60.
[6] E. Fridman and U. Shaked, An improved stabilization method for linear time-delay systems, *IEEE Transactions on Automatic Control* **47**(11) (2002), 1931–1937.
[7] Y.S. Lee, Y.S. Moon, W.H. Kwon and P.G. Park, Delay-dependent robust H_∞ control for uncertain systems with a state-delay, *Automatica* **40**(1) (2004), 65–72.
[8] A. Goubet-Batholomeus, M. Dambrine and J.P. Richard, Stability of perturbed systems with time-varying delays, *Systems & Control Letters* **31**(3) (1997), 155–163.
[9] H.Y. Hu and Z.H. Wang, *Dynamics of Controlled Mechanical Systems with Delayed Feedback*, Springer-Verlag, Berlin, 2002.
[10] M. Abdel-Rohman, Time-delay effects on active damped structures, *Journal of Engineering Mechanics ASCE* **113**(11) (1987), 1709–1719.
[11] L.L. Chung, A.M. Reinhorn and T.T. Soong, Experiments on active control of seismic structures, *Journal of Engineering Mechanics ASCE* **114**(2) (1988), 241–256.
[12] S.M. Greery, T.T. Soong and A.M. Reinhorn, An experimental study of time delay compensation in active structural control, *Proceedings of The Sixth International Modal Analysis Conference SEM* **1** (1998), 733–739.
[13] G.P. Cai, J.Z. Huang and S.X. Yang, An optimal control method for linear systems with time delay, *Computers and Structures* **81**(15) (2003), 1539–1546.
[14] G.P. Cai and J.Z. Huang, Optimal control method for seismically excited building structures with time-delay in control, *Journal of Engineering Mechanics ASCE* **128**(6) (2002), 602–612.
[15] G.P. Cai and L.X. Chen, Delayed feedback control experiments on some flexible structures, *Acta Mechanica Sinica* **26**(6) (2010), 951–965.
[16] L.X. Chen, G.P. Cai and J. Pan, Experimental study of delayed feedback control for a flexible plate, *Journal of Sound and Vibration* **322**(4–5) (2009), 629–651.
[17] H. Masakazu and H.Y. Hu, Using a new discretization approach to design a delayed LQG controller, *Journal of Sound and Vibration* **314** (2008), 558–570.
[18] B. Liu, H. Masakazu and H.Y. Hu, A new reduction-based LQ control for dynamic systems with a slowly time-varying delay, *Acta Mechanica Sinica* **25** (2009) 529–537.
[19] H.P. Du and N. Zhang, H_∞ control for buildings with time delay in control via linear matrix inequalities and genetic algorithms, *Engineering Structures* **30** (2008), 81–92.
[20] P. Chen and Y.C. Tian, Delay-dependent robust H_∞ control for uncertain systems with time-varying delay, *Information Science* **179** (2009), 3187–3197.
[21] C. Alberto, D.M. Giuseppe, N. Ciro and P. Salvatore, Robust control of flexible structures with stable bandpass controllers, *Automatica* **44** (2008), 1251–1260.
[22] L.L. Chung, C.C. Lin and K.H. Lu, Time-delay control of structures, *Earthquake Engineering and Structural Dynamics* **24**(5) (1995), 687–701.
[23] K.V. Yuen and J.L. Beck, Reliability-based robust control for uncertain dynamical systems using feedback of incomplete noisy measurements, *Earthquake Engineering and Structural Dynamics* **32**(5) (2003), 751–770.
[24] Z.C. Qiu, X.M. Zhang, H.X. Wu and H.H. Zhang, Optimal placement and active vibration control for piezoelectric smart flexible cantilever plate, *Journal of Sound and Vibration* **301** (2007), 521–543.
[25] B. Stephen, E.G. Laurent, E. Feron and V. Balakrishnan, Volume 15 of studies in applied mathematics, society for industrial and applied mathematics (SIAM), *Linear Matrix Inequality in System and Control Theory Philadelphia*, 1994, ISBN o-89871-334-X.
[26] K. Gu, A further refinement of discretized Lyapunov functional method for the stability of time-delay systems, *International Journal of Control* **74**(10) (2001), 967–976.
[27] Y.C. Su, C.B. Jiang and Y.H. Zhang, Matrix theory, *Science Press*, Beijing, 2006 (in Chinese).